

## **A Statistical Analysis of Random Noise Signals for Johnson Noise Thermometry**

Byung Soo Moon , In Koo Hwang  
Korea Atomic Energy Research Institute  
P.O.Box 105, Yusong, Daejeon 305-600, Korea

David E. Holcomb  
Oak Ridge National Laboratory  
P.O. Box 2008, Oak Ridge, Tennessee 37831-6010, USA

### **Abstract**

The results of a statistical analysis on the Johnson noise signals, equivalently band pass filtered random signals are described in this paper. We determined an optimal sampling time needed to extract the most information from the cross power spectral density for a given interval of frequency band, showed that the band pass filtered sensor signal and the channel noises are statistically uncorrelated in long term averages, estimated the number of signal blocks for the long-term averages required to meet a desired accuracy, estimated the amount of time required for processing signals to obtain the desired accuracy, and finally showed how accurate is the linearity of the processed signal.

### **I. Introduction**

Johnson noise thermometry is one of the unconventional methods used for an accurate temperature measurement [1], by which one can establish thermodynamic temperature scale up to 1000°C with an accuracy of 0.2%. During the past 30years, there have been many studies and experimental implementations for application of the noise thermometers for hostile environments [2] such as space applications and high temperature reactors. Temperature measurements in space nuclear reactors [3] require an accuracy of 1 to 2% at temperatures up to about 1400K for about 10 years and the Johnson noise thermometry is believed to be able to provide this performance with measurement uncertainty reduced to 0.2% [4]. For high temperature gas reactors, there have been studies on Johnson noise thermometry for reliable in-core temperature measurements [5]. For nuclear power plant applications, ORNL reports that they performed tests in two operating reactors: Diablo Canyon and Sequoyah to obtain inaccuracies of less than 0.1% for ideal situations and 0.5-1% at the ends of long extension cables [6].

In this paper, we describe the results of a statistical analysis performed as a part of the design work for a digital signal processing system to be used for a Johnson noise thermometry. The Johnson noise [7] is a

synonym of the “thermal noise” generated by thermal agitation of electrons in a conductor and is known to be a result of the Brownian motion of ionized molecules within a resistance [8]. The noise power  $P$  in watts is given by  $P = kT\Delta f$ , where  $k$  is Boltzman’s constant in joules per kelvin,  $T$  is the conductor temperature in kelvins, and  $\Delta f$  is the bandwidth in hertz. The thermal noise power has the property that it is equal throughout the frequency spectrum, depending only on  $k$  and  $T$  and hence it can be used to measure the temperature. A random noise with its autocorrelation function zero everywhere but at 0, is called a white noise and the Johnson noise has the same property so that ‘white noise’ is another synonym of the Johnson noise, and we use this fact to study the Johnson noise statistically by generating random signals.

There are a few different methods in implementing the Johnson noise thermometry. We will be using the correlation voltage method which is based on the correlation of signals from two different channels. Let the signals from the two channels be  $\mathbf{f} = \{\mathbf{f}_i \mid i = 1, 2, \dots, N\}$  and  $\mathbf{j} = \{\mathbf{j}_i \mid i = 1, 2, \dots, N\}$ , then one can write  $\mathbf{f}_i = x_i + \mathbf{e}_{1i}$  and  $\mathbf{j}_i = x_i + \mathbf{e}_{2i}$ , where  $x = \{x_i \mid i = 1, 2, \dots, N\}$  is the sensor signal without the channel noise and  $\mathbf{e}_{1i}, \mathbf{e}_{2i}$  are the channel noise signals. As described above, the temperature is a constant multiple of the expected value of  $x^2$ , i.e.  $E(x^2)$ , and if we compute the expectation value of the product of two signals  $\mathbf{f}$  and  $\mathbf{j}$ , then we have

$$E(\mathbf{f}\mathbf{j}) = E((x + \mathbf{e}_1)(x + \mathbf{e}_2)) = E(x^2) + E(x\mathbf{e}_2) + E(\mathbf{e}_1x) + E(\mathbf{e}_1\mathbf{e}_2) \quad \text{-----} \quad (1)$$

Note that  $E(x\mathbf{e}_2)$ ,  $E(\mathbf{e}_1x)$  are expected to be zeros since the noise signal  $\mathbf{e}_1$  or  $\mathbf{e}_2$  and the sensor signal  $x$  are uncorrelated with the means of the noise signals zero. The last term  $E(\mathbf{e}_1\mathbf{e}_2)$  is also zero since the two channel noises are uncorrelated. Therefore, the temperature which is a constant multiple of  $E(x^2)$  can be computed by the same constant multiplied by  $E(\mathbf{f}\mathbf{j})$  if the above assumptions are true.

Using the Parseval’s formula [9],  $E(x^2)$  can be computed by a constant multiple of  $E(\Phi\Psi)$  where  $\Phi$  and  $\Psi$  are the Fourier transformations of  $\mathbf{j}$  and  $\mathbf{y}$  respectively. Note that the channel noises will also be removed in  $E(\Phi\Psi)$ . Thus, we can remove EMI noises not filtered by the band pass filter by using the cross power spectral density  $G(x) = \Phi(x)\Psi(x)$ , where  $\Phi$  and  $\Psi$  are considered as functions of the noise signal  $x$ . Now, suppose we take  $N$  independent samples  $x[n]$  for  $n=1, 2, \dots, N$  and let  $\bar{x}^2[n] = E(x^2[n])$ . Then the average  $\mathbf{t}$  of  $\bar{x}^2[n]$  for  $n=1, 2, \dots, N$  can be written as

$$\mathbf{t} = \frac{1}{N} \sum_{n=1}^N \bar{x}^2[n] = \frac{E(\bar{x}^2)}{N} \sum_{n=1}^N \frac{\bar{x}^2[n]}{E(\bar{x}^2)} = \frac{E(\bar{x}^2)}{N} \mathbf{c}^2(N) \quad \text{-----} \quad (2)$$

where  $\mathbf{c}^2(N)$  is the Chi-square random variable defined by

$$\mathbf{c}^2(N) = \sum_{i=1}^N \left( \frac{x_i - \mathbf{m}}{\mathbf{s}} \right)^2$$

with  $\mathbf{m}$  and  $\mathbf{s}$  being the mean and standard deviation of  $x_i$ ’s.

Note that  $E(\mathbf{t}) = E(\bar{x}^2)$  and hence from (2) the mean of  $\mathbf{c}^2(N)$  is  $N$  so that we have the variance

of  $c^2(N)$  equals  $2N$ , i.e.  $\text{Var}(c^2(N)) = 2N$ . Using the property  $\text{Var}(ay) = a^2 \text{Var}(y)$ , we now have

$$\text{Var}(c^2(N)) = \text{Var}\left(\frac{Nt}{E(\bar{x}^2)}\right) = \frac{N^2}{(E(\bar{x}^2))^2} \text{Var}(t) = 2N.$$

Thus, we have  $\text{Var}(t) = \frac{2}{N} (E(\bar{x}^2))^2$ . Therefore the relative error or the measurement error becomes

$$\frac{s_t}{E(\bar{x}^2)} = \sqrt{\frac{2}{N}} \dots\dots\dots (3)$$

In the following sections, we prove that the above are indeed true for random signals where random signals are of the form  $\sum_a a_a \text{Sin}(2\pi f_a t + w_a)$  with  $a_a$  being a random number in  $[0,1]$ ,  $f_a$  a random integer in  $[3 \times 2^{15}, 1.2 \times 2^{20}]$ , and  $w_a$  a random number in  $[0, 2\pi]$ .

## 2. Determination of the Sampling Time and the Frequency Range

In this section, we consider how the frequency band for filtering the noise data and the necessary sampling time are determined. Ideally, the thermometer should have as wide a bandwidth as possible not only to keep the measurement times short but also to increase the accuracy. If we take a shorter sampling time, then we will have more accurate temperature during the same time interval since our temperature value will be computed by taking the average of long-term fluctuating values. But there are practical limitations. The upper bound of the frequency range is required to eliminate the high frequency EMI associated with AM radio transmissions. The lower bound is set to reduce the EMI due to low frequency magnetic fields, particularly associated with the power supplies. A survey by D. white et al. [8] shows that the typical frequency range used is from a few kilohertz to one megahertz. The size of the frequency band and the number of points in the sampling block determine the resolution of the Fourier transformation.

We assume that the number of sample points in a block of samples is 1024 points. This limitation comes from the fact that the FFT algorithm we will be using for a set of 1024 points requires 6M gates while the FPGA board we designed initially has only 15M gates. First, we consider the case where the sampling time is 16MHz, i.e.  $h = \frac{1}{2^{24}}$  sec, which is practically the fastest rate currently, considering the fact that 12 Bit A/D conversion must be used. Note that there must be more than two points, i.e. three or more points in one period of a signal so that the amplitude of the signal after the Fourier transformation is properly reflected in the frequency domain. Thus, if we require four points to be the minimum, then the signal with  $4h = \frac{1}{2^{22}}$  sec as one cycle time will have the minimum period and hence the maximum frequency of  $2^{22}$  (4MHz). In a set of 1024 sample data, there will be 256 cycles for these signals of

frequency  $2^{22}$  (4MHz). Therefore, the amplitudes after FFT of frequencies corresponding to 257 through 512 are wasted. For the lower limit, note that input signals of frequency  $2^{17}$  (128kHz) will be transformed to 8 since there are 8 cycles of such signals in 1024h second time period.

However, the signals we get from the preamplifiers fabricated by Oak ridge National Laboratory initially have frequencies below 1.5MHz and the amplitudes of the frequencies in the range 100kHz to 1.2MHz can be read properly after nonlinear gain correction. Thus, we decided to lower the sampling period to  $h = \frac{1}{3 \times 2^{20}}$  sec. Note that for signals of frequency 1.2MHz, one period will be  $\frac{1}{1.2 \times 2^{20}}$  sec, which is 2.5h. Therefore, two or more points will be sampled from each cycle. Now, consider signals of frequency 3kHz =  $3 \times 2^{10}$  cycles/sec whose period will be  $\frac{1}{3 \times 2^{10}}$  sec. One block of 1024 sample points will correspond to a time interval of length  $2^{10} h = \frac{1}{3 \times 2^{10}}$  sec, which is the same as the one cycle length of 3kHz signals, and hence 3kHz signals will be transformed to 1 by the Fourier transformation. Thus, if we take  $3 \times 2^5$  kHz = 96kHz be the lower bound of the filter, then the lower bound 96kHz will be transformed to 32 while the upper bound 1.2MHz will be transformed to about 410. Therefore, we will be using the frequency range [32, 410]. Fig.1 shows the power spectral density of a sample Johnson noise signal filtered in the range  $[3 \times 2^{15}, 1.2 \times 2^{20}]$ . Note that the values of the spectral density near 32 and 410 are smaller than those at interior points. In the next section, we consider the energy leakage problem at the boundary frequencies 32 and 410.

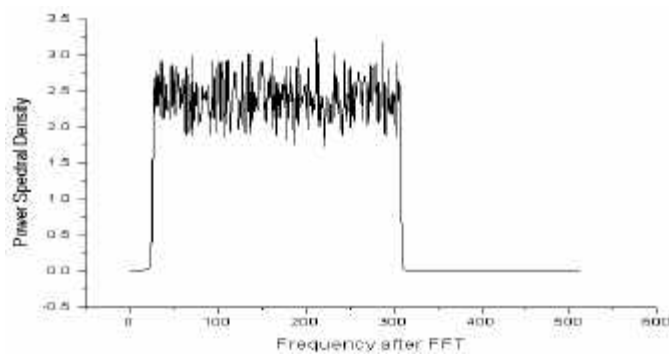


fig.1. Power Spectral Density of a Sample Johnson Noise

### 3. Energy Leakage Problem at Boundary Frequencies

Since the signals are windowed by a frequency band, the power of the original sequence  $\{x(i)\}$  concentrated at a single frequency will spread by the window into the entire frequency range, which is called energy leakage. The left hand side graph of fig.2 shows an example of the Fourier transform of

$\{x(i) = \text{Sin}(2\pi f t_i) | i = 1, 2, \dots, 1024\}$  with  $f = 3 \times 2^{16} - 3 \times 2^9$  and  $t_i = \frac{i-1}{3 \times 2^{20}}$ . Recall that the signals with frequency  $3 \times 2^{10}$  will be transformed to 1 and hence signals with frequency  $3 \times 2^{16}$  will be transformed to 64 and the Fourier transformation of the signal with single frequency  $3 \times 2^{16} - 3 \times 2^9$  will have the mean at 63.5 as shown in fig.2.

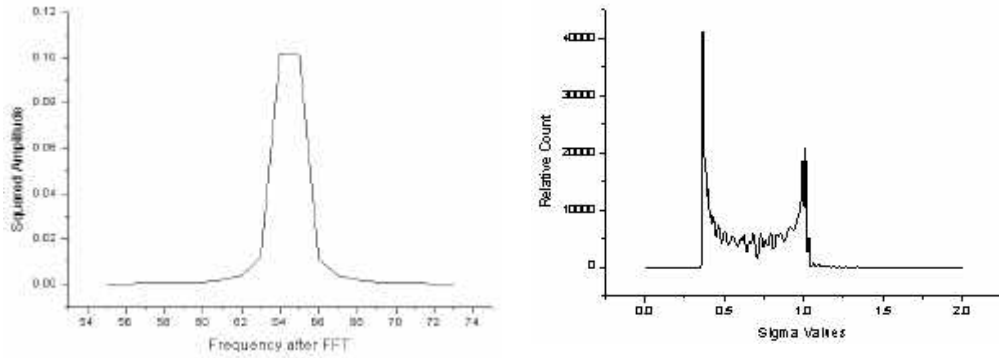


fig.2. Transformed Freq. Distribution for a Single Freq. Input (Left) and Sigma Values for Transformed Single Frequency Signals (Right)

As described in section 1, the temperature can be computed by a constant multiple of the average of the cross power density spectrum in the frequency domain. Since only the frequencies in a fixed range of frequencies will pass through the band pass filter described above and the Fourier transformation of the single frequency signals in the band will mostly spread, there will be “energy leakages”. To determine how much of the power will be “leaked out” at the boundary frequencies, we computed the following:

- (1) Take a signal  $f(t) = \text{Sin}(2\pi w t)$  with the frequency  $w$  in the interval  $[3 \times 2^{15}, 1.2 \times 2^{20}]$  and  
 Compute  $f_i = f(t_i), i = 1, 2, \dots, 1024$  with  $t_i = \frac{i}{3 \times 2^{20}}$
- (2) Compute the Fourier transformation of  $\{f_i | i = 1, 2, \dots, 1024\}$  to obtain  $\{g_i | i = 1, 2, \dots, 1024\}$  where  $g_i$  are the magnitude of the complex numbers
- (3) Considering  $\{g_i^2 | i = 1, 2, \dots, 1024\}$  as a probability distribution, compute the mean and sigma of this distribution
- (4) Repeat the above process for all the frequencies ranging from  $3 \times 2^{15}$  to  $1.2 \times 2^{20}$  and plot how the means are distributed.

The result of calculation is shown in the right hand side graph of fig.2, where the sigma values ranges from 0.3 to 1.0 with the mean at 0.669. Note that we may take  $0.669 + 3 \times 0.234 = 1.339$  as the maximum span of the “leakage” and hence if any of the frequencies in the range  $[34, 408]$  will not have any ‘leakage’. Note that the leaked out energy at 34 will be at 33 or below and hence the average of the power spectral density at interior points will be proportional to the temperature.

#### 4. Channel Noise

In this section, we consider the effect of the noise picked up in the long channel cables from the amplifier to the A/D converter where the temperature is calculated. As described in Section 1, let the signals from the two channels be  $\mathbf{f} = \{f_i | i=1,2,\dots,N\}$  and  $\mathbf{j} = \{j_i | i=1,2,\dots,N\}$ , and write  $f_i = x_i + e_{1i}$  and  $j_i = x_i + e_{2i}$ , where  $x = \{x_i | i=1,2,\dots,N\}$  is the sensor signal without the channel noise and  $e_{1i}, e_{2i}$  are the channel noise signals. Consider the expectation value of the product of two signals  $\mathbf{f}$  and  $\mathbf{j}$ , i.e.

$$E(\mathbf{f}\mathbf{j}) = E((x + \mathbf{e}_1)(x + \mathbf{e}_2)) = E(x^2) + E(x\mathbf{e}_2) + E(\mathbf{e}_1x) + E(\mathbf{e}_1\mathbf{e}_2) \quad \text{-----} \quad (1)$$

In the following, we will examine how large are the values  $E(x\mathbf{e}_2)$ ,  $E(\mathbf{e}_1x)$ , and show that  $E(\mathbf{e}_1\mathbf{e}_2)$  approach to zero faster than the rate  $\sqrt{\frac{2}{N}}$  which is the relative error for  $E(x^2)$ . We will assume that the

channel noises are of the same form as the Johnson noise except that the channel noise is not filtered and that they are sums of much less number of single random frequency signals. For the signal  $x$ , we used signals of the form  $x(t) = \sum a \times \sin(2\pi ft + b)$  with the amplitude  $a$  being a random number in  $[0,1]$ , the phase angle  $b$

also a random number in  $[0,2\pi]$ , and the frequency  $f$  is a random integer in  $[3 \times 2^{15}, 1.2 \times 2^{20}]$ . For the sampling time, we use  $h = \frac{1}{3 \times 2^{20}}$  so that  $x_i = f\left(\frac{i}{3 \times 2^{20}}\right)$ , for  $i=1,2, \dots, 1024$ . As will be described in

Section 5, the number of terms in the sum of  $f(t)$  determines the temperature so that smaller number of terms will correspond to a lower temperature. The left hand side graph of fig.3 shows the power of a signal  $\{x_i | i=1,2,\dots,1024\}$  obtained from sums of 4096 random single frequency signals after taking the average of 64 blocks. For the channel noise signals  $\{y_i | i=1,2,\dots,1024\}$ , we used the similar function  $f(t)$  with the number of added single frequency signals range from 1 to 64, and 1000 to 1200. The right hand side graph of fig.3 shows the power of a noise signal obtained by averaging 64 noise signals each with a single frequency, a sum of two single frequencies, a sum of three single frequencies, and so forth. When the correlation coefficient  $c$  between the two sequences  $\{x_i\}$  and  $\{y_i\}$  are computed,

$$c = \frac{\sum x_i y_i}{\sqrt{\sum x_i^2 \sum y_i^2}}$$

we find that  $c$  ranges from 0.028 to 0.038 while mean of the signal powers range from 675 to 686. When average of 4096 blocks (see fig.5) is taken, the correlation coefficient decreases to 0.00004 while the signal power remains to be the same. When the noise is a sum of  $2^{15}$  random single frequency signals, the correlation coefficient is found to be around 0.0006 that is still far below the desired relative error for the

signal power, i.e.  $\sqrt{\frac{2}{4096}} = \frac{\sqrt{2}}{64} = 0.022$ . Therefore, we may consider the random noise signals and the sensor signals are uncorrelated.

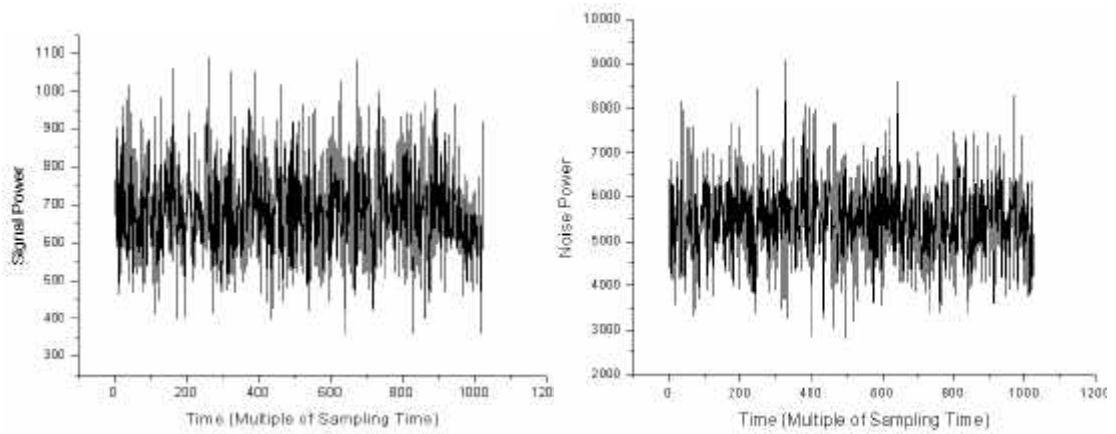


fig.3. Signal Power of a Sample Voltage Signal and Power of a Sample Noise Signal (Avg. of 64Blocks)

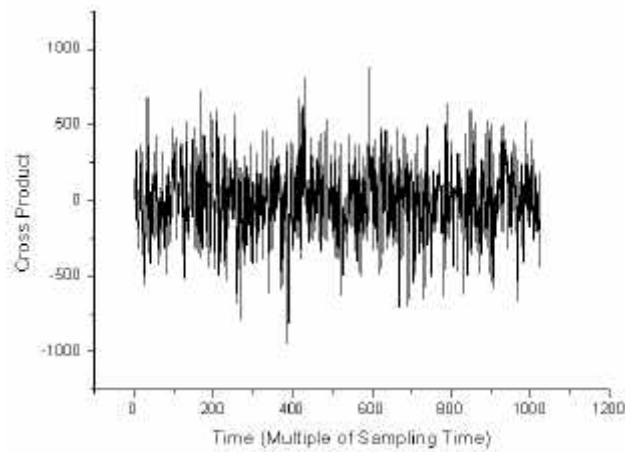


fig.4. Cross Product of a Sample Noise and the Sensor Signal (Avg. of 64Blocks – Correlation Coefficient is 0.03)

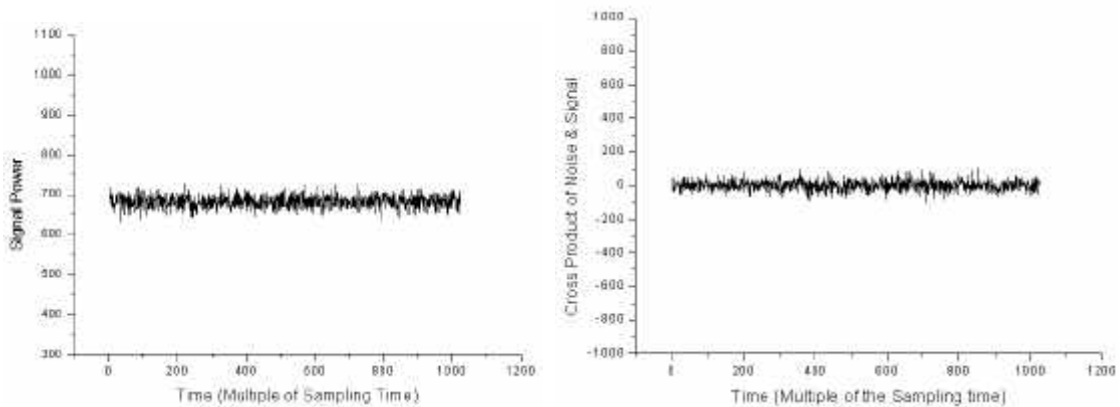


fig.5. Signal Power (left) and Cross Product of Noise and the Signal (right) (Average of 4096Blocks – Corr. Coeff. is 0.0006)

## 5. Linearity of the Processed Signal Power

In this section, we study how the signal power or equivalently the power spectral density increases as the number of random signals summed to form the Johnson noise increases. We performed calculations for the functions obtained by summing  $2^{11}$ ,  $2^{12}$ , ...,  $2^{18}$  single frequency random signals with the frequencies in the range  $[3 \times 2^{15}, 1.2 \times 2^{20}]$ . Table 1 shows a summary of the results where the first two rows are the means and the sigmas of the averaged signal power while the remaining two rows are for the power spectral density.

**Table 1. Average of Signal Power and Power Spectrum Density**

No of Signals	$2^{11}$	$2^{12}$	$2^{13}$	$2^{14}$	$2^{15}$	$2^{16}$	$2^{17}$	$2^{18}$
Sigma( SP)	341.129	682.232	1365.417	2732.603	5468.062	10914.70	21800.38	43663.86
Sigma( SP)	15.005	30.456	58.799	122.948	233.322	445.624	889.649	1797.51
Mean(PSD)	0.45116	0.90241	1.80599	3.61388	7.23178	14.43632	28.83659	57.74675
Sigma(PSD)	0.01536	0.03250	0.06013	0.12422	0.22321	0.46009	0.95255	2.00390

The computed results in Table 1 are drawn by graphs shown in fig.6. The left hand side graph of fig.6 shows the means of the signal power in the middle curve that is almost a straight line. The two other curves surrounding the middle curve are drawn so that they reflect the one-sigma band. Similarly, the right hand side graph of fig.6 is drawn for the power spectral density in Table 1. Fig.7 is another schematic illustration of the linearity shown in Table 1 with the Gaussian functions center at the means and with the sigmas as the standard deviations.

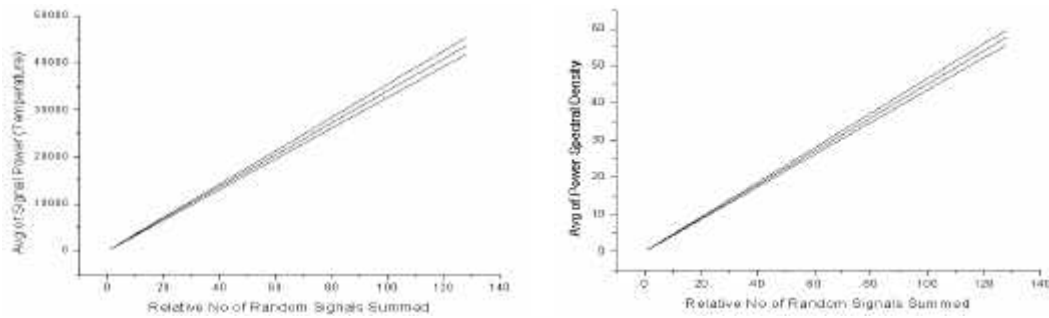


Fig.6. Linearity of Johnson Noise Signals with One Sigma Band -1  
(Average of 1024 Blocks)

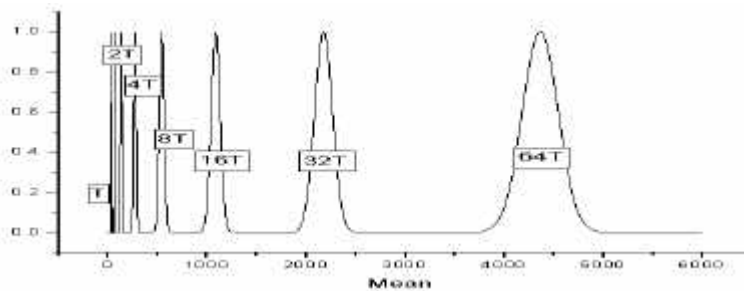


Fig.7. Linearity of Johnson Noise Signals with One Sigma Band -2



## 6. Measurement Uncertainty and Moving Average Problems

In this section, we describe the results of calculations performed to verify the error estimates (3) described in Section 1 and the results of an analysis to determine the amount of changes expected by replacing the averages by the moving averages. The two graphs in Fig.8 and the two graphs in fig.10 show an example on how the signal power changes as the number of blocks used in taking the averages increases. All of the two graphs in fig.8 and the two graphs in fig.10 show a random signal obtained by taking a sum of 1024 single frequency signals with frequencies in the range  $[3 \times 2^{15}, 1.2 \times 2^{20}]$ . The first graph in fig.8 is obtained by taking an average of 64 blocks, the second is an average of 1024 blocks, the first in fig.10 is an average of  $2^{14}$  blocks, and the second in fig.10 is an average of  $2^{18}$  blocks. Each of the blocks consist of 1024 sampled points and each point is sampled at  $\frac{1}{3 \times 2^{20}}$  sec intervals. The two figures fig.9 and fig.11 show the corresponding power spectral density curves.

**Table 2. Relative Error vs the Number of Blocks used for Averages (Sum of  $2^{11}$  random signals)**

No of Blocks	Average of Signal Power			Average of Spectral Power Density		
	Mean	Sigma	Sigma/Mean	Mean	Sigma	Sigma/Mean
64	340.802	58.702	0.17225	0.45070	0.06156	0.13658
1024	341.129	15.005	0.04399	0.45150	0.01515	0.03356
16384	341.309	3.7120	0.01088	0.45171	0.00396	0.00867
262144	341.298	0.7850	0.00230	0.45168	0.00122	0.00270

**Table 3. Relative Error vs the Number of Blocks used for Averages (Sum of  $2^{12}$  random signals)**

No of Blocks	Average of Signal Power			Average of Spectral Power Density		
	Mean	Sigma	Sigma/Mean	Mean	Sigma	Sigma/Mean
64	685.194	124.93	0.18233	0.90625	0.12115	0.13367
1024	682.232	30.456	0.04664	0.90335	0.03092	0.03428
16384	682.104	7.209	0.01057	0.90268	0.00822	0.00911
262144	682.703	1.776	0.00260	0.90348	0.00316	0.00350

Table 2 shows a summary of the calculated results for random noise signals that are sums of 2048 single frequency signals. A total of 262,144 blocks of 1024 points each are generated and the means and sigmas for 64 blocks,  $16 \times 64$  blocks,  $16 \times 16 \times 64$  blocks,  $16 \times 16 \times 16 \times 64$  blocks are shown. The relative errors defined as the ratio of sigma over the mean are shown in column 4 for the signal power, and in column 7 for the power spectral density. One can draw a conclusion from these ratios that the relation (3) in section 1 is true. It is apparent from Table 3 that the same holds for the case when the noise signals are sums of 4096 single frequency signals.

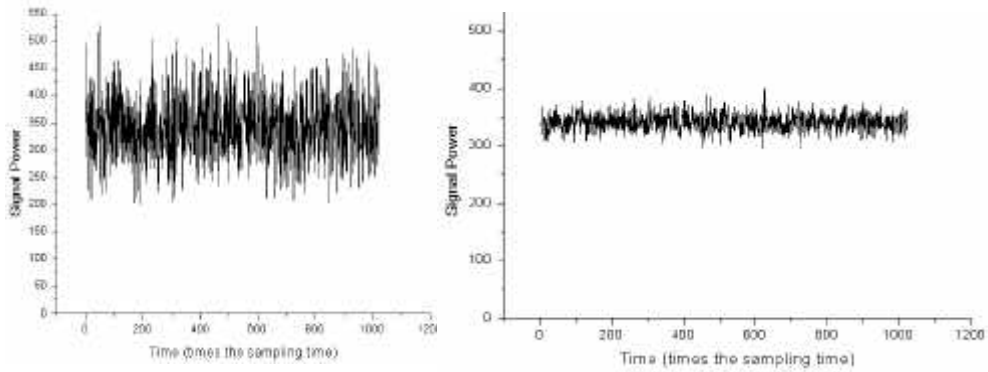


Fig.8. Signal Power (Left - Average of  $2^6$  Blocks ;  $m = 340.802, s = 58.702$   
 Right -Average of  $2^{10}$  Blocks;  $m=341.129, s=15.005$  )

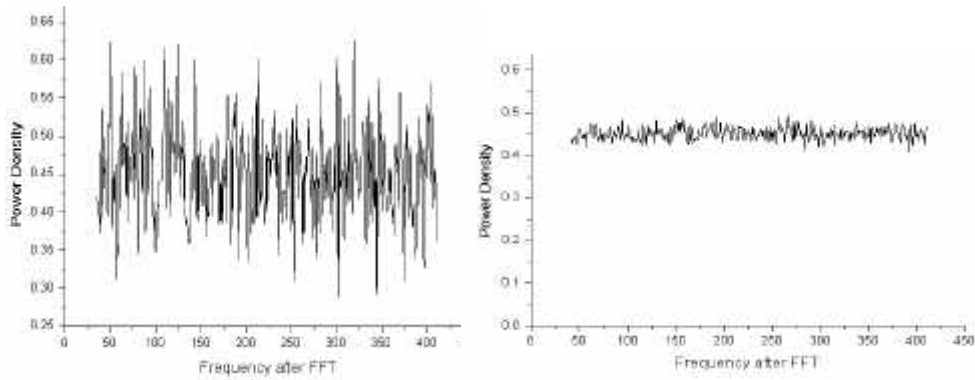


Fig.9. Power Density Spectrum (Left - Avg. of  $2^6$  Blocks ;  $m = 0.45070, s = 0.06156$   
 Right -Avg. of  $2^{10}$  Blocks;  $m = 0.45116, s = 0.01536$  )

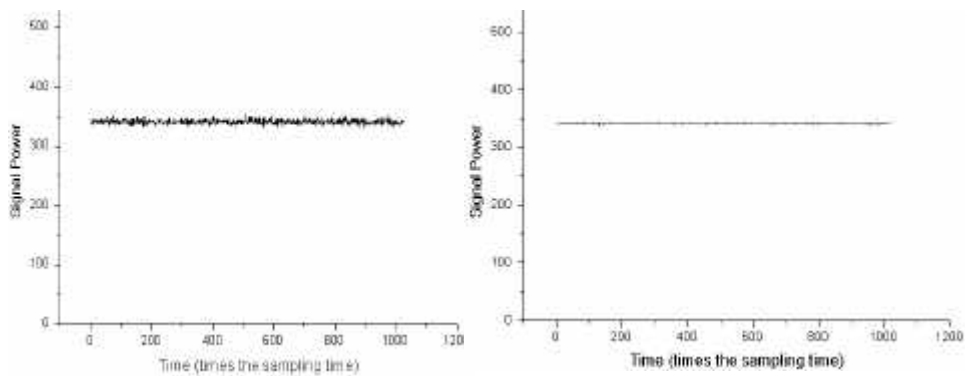


Fig.10. Signal Power (Left - Average of  $2^{14}$  Blocks;  $m = 341.309, s = 3.712$   
 Right - Average of  $2^{18}$  Blocks;  $m = 341.298, s = 0.785$  )

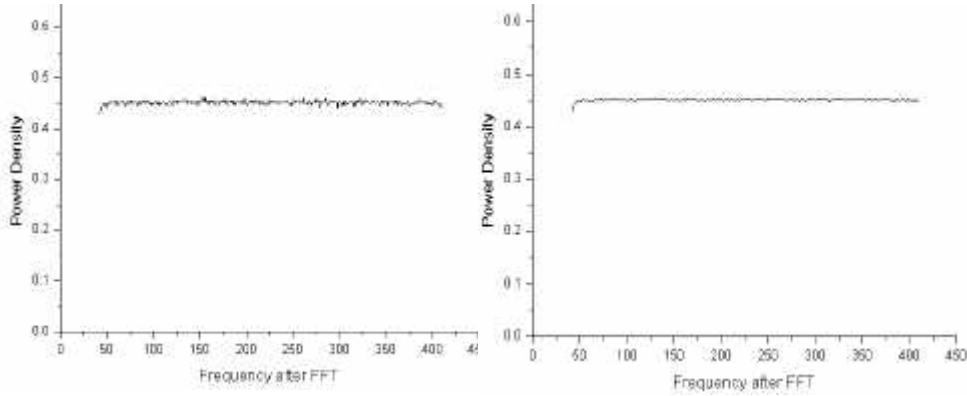


Fig.11. Power Density Spectrum (Left – Avg. of  $2^{14}$  Blocks ;  $m = 0.45144, s = 0.00458$   
Right –Avg. of  $2^{18}$  Blocks;  $m = 0.45141, s = 0.00271$ )

Next, we consider the problem of replacing the averages by the moving averages. As seen above, the high accuracy of the Johnson noise thermometer is achieved through taking a long average of the signal power. To obtain an accuracy of 0.28%, however, one quarter of a million blocks of samples are needed to be averaged so that a storage of  $250,000 \times (410-32)$  floating numbers are needed to store the power spectral density obtained though FFT. To avoid this large storage area and to avoid the necessary I/O time, one must use a moving average algorithm.

Assume that we want to take an average of  $N$  terms in a time sequence  $\{x_n\}$ . Let  $a_{m-1}$  be the moving average using the values up through  $x_{m-1}$ . Then with the value  $x_m$ , the new average  $a_m$  will be computed by  $a_m = (1-h)a_{m-1} + hx_m$ , where  $h = \frac{1}{N}$ . Repeating the same, the next average is computed as  $a_{m+1} = (1-h)^2 a_{m-1} + h(1-h)a_m + hx_{m+1}$ . In general, we have

$$a_N = a_0 + h \sum_{i=1}^N (1-h)^{i-1} x_{N+1-i}$$

To compute how large is the contribution by  $\{x_{-i} \mid i = 0,1,2,\dots\}$ , we assume that the temperature is steady, i.e.

$x_i = x_j$  for all  $i$  and  $j$ . Then the multiplier in the sum of the last  $N$  terms will be  $h \sum_{i=1}^N g^{i-1} = 1 - g^N$ , where

$g = 1-h$ . Therefore, the remaining sum will be  $g^N = \left(1 - \frac{1}{N}\right)^N$  whose limit as  $N \rightarrow \infty$  is

$e^{-1} = 0.36787944$ . The results of sample calculations for  $N=2^{10}, 2^{16}, 2^{20}$  are; when  $N=2^{10}$  we have  $g^N = 0.3677$ ,  $g^{5N} = 0.00672$ ,  $g^{6N} = 0.000247$ , and when  $N=2^{16}$ , we have  $g^N = 0.3679$ ,  $g^{5N} = 0.00674$ ,  $g^{6N} = 0.000248$ , and they are almost the same for  $N=2^{20}$ . The coefficients of  $x_N, x_{N-2^{13}}, x_{N-2 \times 2^{13}}, x_{N-7 \times 2^{13}}, x_{N-8 \times 2^{13}}$  are found to be  $0.152588E-4, 0.118835E-4, 0.104872E-4, 0.925489E-5, 0.816740E-5, 0.720770E-5, 0.636077E-5, 0.561472E-5$  respectively. The ratio of the  $65,536^{\text{th}}$

coefficient relative to the most recent is 0.3678822, i.e. about 36%. Thus, we conclude that if we use four to five times larger number of blocks, then we can achieve nearly the same accuracy by using the moving averages provided that the temperature is steady. The result of a sample calculation to verify this is omitted.

## 7. Accuracy vs the Processing Time

In this section, we consider how much time is needed to compute the long-term averages of the cross-power spectral density. Assume that we need an accuracy of 0.28% that is equal to  $\sqrt{\frac{2}{250000}}$  so that the number of blocks required is one quarter of a million by (3). We further assume that the sampling rate is  $\frac{1}{2^{24}}$  sec, which is practically the fastest A/D conversion time currently assuming that 12bit accuracy is used.

The largest number of blocks that can be sampled in 1 second would then be  $2^{14}$  so that sampling  $2^{18}$  blocks (one quarter of a million blocks) would require 16seconds. On the other hand, for the process time whose major component is the FFT algorithm, we need to compute the time required to do one FFT algorithm. To do an FFT of 1024 points, one can count easily that there are 75,796 multiplications or divisions, 95,282 additions or subtractions, and 20,480 evaluations of the Cosine or Sine function. With a 2.8GHz Pentium-IV processor using FORTRAN, one can perform  $10^8$  multiplications,  $4 \times 10^8$  additions, about  $10^7$  evaluations of the Sine or Cosine function separately with no type conversions of variables such as from integer to real is used. Therefore, using these one can compute that an FFT takes  $20,480 \times 10^{-7} + 75,796 \times 10^{-8} + 95,282 \times 10^{-8} / 4.4 = 0.00302$  sec, so that about 330 FFT's can be performed in 1 second. In our development, we will be using Xilinx gate arrays so that more FFT's can be performed in 1 second. How many FFT's can be done in 1 second will depend not only on the number of gates used but also on the type of gate arrays. Note that no matter how fast the FPGA's would do the FFT, the limit of 16 seconds sampling time would still be there. However, for nuclear power plant applications, the maximum RCS temperature change during the normal operation is 27°C/hr (0.008°C/sec=0.48°C/Min) due to the operation limit specified in the technical specification. Note that 0.48°C is below 0.28% of 310°C and hence the change in 1 minute is within the accuracy range of our Johnson noise thermometer.

## 8. Conclusion

We have verified through a statistical analysis that the Johnson noise thermometer can be used to improve the measurements of the RCS temperature within an accuracy of below 0.28%, provided that the necessary computation speed can be achieved by using FPGA's. Some of the design parameters for a design of the FPGA processing board have been determined through this study. The shapes of signal power curves shown by various figures in this paper differ from the ones for the real signals in that the latter curves are not as flat

as the former. This is due to the fact that the band pass filter does not work as ideal as one would expect. This problem can be handled properly by nonlinear gain correction where the correction factors are obtained from a continuous calibration signal. Another difference between the real signals and our random signals is that the real signals have EMI noises picked up in the channels. We expect that these EMI noises can be cut off properly by using the power spectral density of the sensor signal.

## References

1. Herman A. Tasman, Joseph Richter, "Unconventional methods for measuring high temperatures", High Temperatures – High Pressure 11 (1979) 87-101.
2. Dimitrios C. Agouridis, "Noise Thermometers for Hostile Environments: A Theoretical Evaluation", IEEE Trans. On Instrumentation and Measurements, 39(5) (1990) 780-784.
3. M. J. Roberts, T. V. Blalock, and R. L. Shepard, "Application of Johnson Noise Thermometry to Space Nuclear Reactors", Space Nuclear Power Systems (1989) 87-93.
4. R. L. Shepard and J. M. Weiss, "Use of SP-100 Thermometry Technology to Improve Operation of Electric Power Plants", Proc. 31<sup>st</sup> Intersociety Energy Conversion Eng. Conf. (1996) 114-118.
5. H. Brixy, R. Hecker, J. Jehmen, P. Barbonus, R. Hans, "Temperature Measurement: Development Work on Noise Thermometry and Improvement of Conventional Thermocouples for Applications in Nuclear Process Heat", Proc. Specialist Meeting on Gas Cooled Reactor Core and High Temperature Instrumentation, Windermere, England (IAEA-TC-389/6-7).
6. R. L. Shepard, et al., "In Situ Calibration of Nuclear Plant Platinum Resistance Thermometers Using Johnson Noise Methods", EPRI NP-3113, Project 1440-1 (1983).
7. <http://glossary.its.bldrdoc.gov/fs-1037/dir-037/5417.htm>
8. D.R. White, R. Galleano, A. Actis, et al., "The status of Johnson noise thermometry", Metrologia 33(4) (1996) 325-335.
9. John G. Proakis and Dimitris G. Manolakis, "Digital Signal Processing, Principles, Algorithms, and Applications", MacMillan Publishing Co. (1992).